H2O Transmission Rate Through Polyethylene Naphthalate Polymer Using the Electrical Ca Test.

ARTICLE *in* THE JOURNAL OF PHYSICAL CHEMISTRY A · JULY 2013

Impact Factor: 2.69 · DOI: 10.1021/jp4043057 · Source: PubMed

4 AUTHORS, INCLUDING:

Jacob Andrew Bertrand
Maxima Sciences LLC
13 PUBLICATIONS **327** CITATIONS
SEE PROFILE

Daniel James Higgs
University of Colorado Boulder
2 PUBLICATIONS **8** CITATIONS
SEE PROFILE

Matthias Young
National Institute of Standards and Technolog…
9 PUBLICATIONS **39** CITATIONS
SEE PROFILE

THE JOURNAL OF PHYSICAL CHEMISTRY A

Article

pubs.acs.org/JPCA

H_2O Vapor Transmission Rate through Polyethylene Naphthalate Polymer Using the Electrical Ca Test

J. A. Bertrand,[†] D. J. Higgs,[†] M. J. Young,[‡] and S. M. George*[,†,§]

[†]Department of Chemistry and Biochemistry, [‡]Department of Chemical and Biological Engineering, and [§]Department of Mechanical Engineering, University of Colorado, Boulder, Colorado 80309-0215, United States

ABSTRACT: The electrical Ca test was used to measure H_2O vapor transmission through polyethylene naphthalate (PEN) polymer with a thickness of 200 μm. On the basis of the time required for the normalized conductance of the Ca film to reach zero, the H_2O vapor transmission rate was determined versus H_2O flux, temperature, and saturation of the PEN polymer with H_2O. The H_2O vapor transmission rate was proportional to the H_2O flux and only weakly dependent on temperature at constant H_2O flux. The transmission coefficient, Γ, for H_2O through the PEN polymer at 70 °C was $\Gamma \sim 3.2 \times 10^{-10}$. The corresponding water vapor transmission rate (WVTR) at 70 °C/80% RH was 0.65 g/(m^2 day). The temperature dependence of the H_2O vapor transmission rate through PEN at constant H_2O flux yielded an activation barrier of E = 12.4 kJ/mol. There was no observable reservoir effect for H_2O in the PEN polymer. The H_2O vapor transmission rates for initially dry or H_2O-saturated PEN polymer substrates were nearly identical at various temperatures. Although the time required for the normalized conductance of the Ca film to reach zero was inversely proportional to the H_2O flux, the Ca film conductance did not decrease linearly versus H_2O exposure. The Ca film conductance changed very little during initial H_2O exposure. This behavior may be caused by the nonlinear oxidation kinetics of the Ca film.

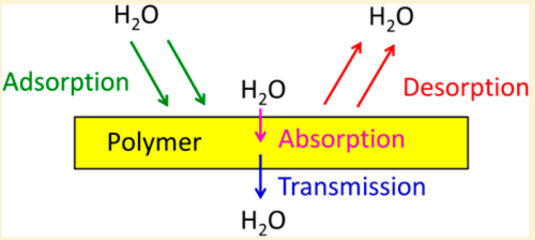

1. INTRODUCTION

The transmission of water through polymers is important in many polymer applications including the packaging of food, medicines, and organic electronics. The transmission rate of a polymer is determined by the permeability multiplied by the pressure and divided by the polymer thickness. According to the solution-diffusion model,[1] the permeability, P, is determined by the product of the diffusivity and solubility, i.e., $P = DS$, where D is the diffusion coefficient and S is the solubility. The diffusion coefficient is a kinetic parameter, and the solubility is a thermodynamic parameter. The diffusion coefficient will be influenced by local activation barriers for H_2O migration in the polymer. The solubility will be affected by the interaction energy between H_2O and the polymer.

The diffusion coefficients and solubilities are not known for many different gaseous molecules in various polymers. Because of the importance of water, there have been measurements of H_2O permeability through a wide range of polymers.[2−9] H_2O permeabilities vary widely from 12 barrer in polyethylene[3] to 40 000 barrer in polydimethylsiloxane.[2] (1 barrer = 10^{-10} (cm^3 (STP) cm)/(s cm^2 cm Hg) where STP is standard temperature and pressure.)[10] The differences in permeabilities reflect the underlying diffusion coefficients and solubilities for H_2O in these polymers. At high H_2O concentrations, water also adds complexity because of its strong hydrogen bonding that leads to H_2O clustering and a lower H_2O permeability.[4,6,8]

Polyethylene naphthalate (PEN) is an optically clear polyester polymer that has been targeted as the substrate for flexible organic light-emitting diodes (OLEDs).[11] To our knowledge, there are no peer-reviewed literature water vapor transmission rate (WVTR) values reported for PEN. However, H_2O permeability in PEN is known to be reasonably high and PEN requires a gas diffusion barrier to be useful for OLED applications.[11] Without the gas diffusion barrier, H_2O will oxidize the low work function metals used in the cathodes of OLED devices. Al_2O_3 coatings grown using atomic layer deposition (ALD) on PEN have been demonstrated to be very effective gas diffusion barriers. WVTRs of $\leq 5 \times 10^{-5}$ g/(m^2 day) at 38 °C/85% RH have been reported for Al_2O_3 ALD coatings on PEN substrates.[12,13] These low WVTRs are close to the ultralow WVTRs of $\sim 10^{-5}$ to 10^{-6} g/(m^2 day) that are required for OLEDs on polymers.[14]

There are no standard testing methods that can measure ultralow WVTRs. The commercial MOCON test is capable of measuring WVTRs only as low as 5×10^{-4} g/(m^2 day). The "Ca test" is one custom method that has been employed to measure ultralow WVTRs. The calcium test uses a thin, metallic, Ca layer as a sensor to measure water vapor transmission rates.[15−17] The Ca film can be monitored as the opaque, metallic Ca film oxidizes to transparent and electrically insulating calcium hydroxide [$Ca(OH)_2$].[18,19] The electrical conductance of the Ca film can be used to measure the Ca film oxidation.[17] The optical transmittance of the Ca film can also be utilized to characterize the extent of Ca film oxidation.[16]

Special Issue: Curt Wittig Festschrift

Received: May 1, 2013
Revised: July 12, 2013

   dx.doi.org/10.1021/jp4043057 | J. Phys. Chem. A XXXX, XXX, XXX−XXX

Other versions of the Ca test involve measuring the oxidized area of the Ca film.[15] The Ca test has been employed by many investigators to measure WVTRs.[12,13,15−17,20−24]

In this study, the H_2O vapor transmission rate through PEN polymer with a thickness of 200 μm was measured using the electrical Ca test. Initial experiments measured the H_2O vapor transmission through the PEN polymer with an Al_2O_3 ALD diffusion barrier. Because the electrical conductance did not decrease linearly versus H_2O exposure, additional experiments explored the PEN polymer by itself. The H_2O vapor transmission rate through the PEN polymer was measured versus H_2O flux at constant temperature. The H_2O vapor transmission through the PEN polymer is expected to scale linearly with H_2O flux if the H_2O molecules do not cluster or alter the PEN polymer.

The H_2O vapor transmission rate was also measured versus temperature at constant H_2O flux. The temperature dependence of the H_2O vapor transmission reveals details about the kinetics of H_2O adsorption, desorption, absorption, and transport through the PEN polymer. The H_2O vapor transmission rate was also determined versus saturation of the PEN polymer with H_2O at different relative humidities. These measurements assess whether there is a H_2O reservoir in the PEN polymer. These studies help to understand H_2O vapor transmission through PEN polymer with and without an Al_2O_3 ALD diffusion barrier and reveal characteristics of the electrical Ca test versus H_2O exposure.

2. EXPERIMENTAL SECTION

A. Preparation of Ca Films and Polymer Samples. The Ca films were prepared on 3 in. × 1 in. glass slides. The slides were first base-bathed to remove any oils and then washed with water, acetone, and methanol. They were left in the methanol bath and placed under a HEPA particle hood where they were subsequently blown dry with filtered N_2. Double-sided tape was then used to attach stainless steel masks to the glass slides. The masks covered a 0.5 in. strip down the center of the glass slide, leaving a 0.25 in. section on either side to be coated with chromium (Cr) metal. Multiple masked slides were then attached to a sample platter that was placed inside a physical vapor deposition (PVD) chamber. This PVD chamber attached to a glovebox has been described previously.[25]

Chromium metal was deposited by sputtering using 400 W of forward power with a 15 mTorr partial pressure of Ar for 20 min. These conditions produced a Cr contact thickness of ~540 nm. The glass slides were then removed, unmasked, and visually inspected for contact uniformity. The coated slides were washed with acetone and methanol to remove adhesive residue. After being blown dry, they were then cut into three 1 in. × 1 in. squares and placed in the N_2 glovebox for Ca deposition.

Immediately prior to each Ca test run, one of the 1 in. × 1 in. glass squares was placed on a custom PVD sample platter and masked to produce a 0.75 in. × 0.5 in. area for Ca deposition. The platter was then inserted into the PVD chamber from the glovebox via a transfer arm and gate valve. Calcium films were deposited using 300 W of forward power with a 15 mTorr partial pressure of Ar. Ca deposition times were typically ~10 min. These conditions deposited a Ca film with a thickness of 275 nm as determined by focused ion beam (FIB) scanning electron microscopy (SEM) measurements. The thickness was 275 ±15 nm on the basis of five separate FIB-SEM measurements. The Ca-coated glass squares were then returned to the N_2 glovebox for assembly into the Ca test apparatus.

X-ray photoelectron spectroscopy (XPS) analysis revealed that the Ca films contained 20 at. % oxygen.[25] For these XPS measurements, Ca was sputtered onto a glass slide using a mask to define the Ca film. A protective Cr film was then sputtered onto and around the Ca film using a larger mask. This Cr film protected the Ca film from direct exposure to atmosphere. The sample was then removed from the glovebox and placed in the XPS instrument. Argon was used to sputter through the protective Cr film and XPS data was then obtained from the Ca film. The XPS signals showed a consistent value of 20 at. % O throughout the Ca film from the protective Cr film to the glass substrate.

The PEN polymer samples were Teonex Q65F from DuPont Teijin Films with a thickness of 200 μm (8 mil). The polymer samples were defined using a custom die to cut circles from a sheet of the PEN polymer. The polymer sheet was stored in the H_2O/O_2-free glovebox. The polymer samples were immediately returned to the glovebox after cutting and stored until needed for the experiments.

B. Ca Test Apparatus. The Ca test apparatus was designed to (1) measure the electrical conductance of the Ca film with minimal residual H_2O in the apparatus and (2) prevent H_2O ingress that did not pass through the polymer substrate. A top view of the Ca film sensor is shown in Figure 1. A side view of the Ca test apparatus is displayed in Figure 2. The Ca test apparatus consisted of a base flange, an electrical flange, an adapter flange, a sample cover flange (small flange and outer ring), and a Ca sensor and holder.

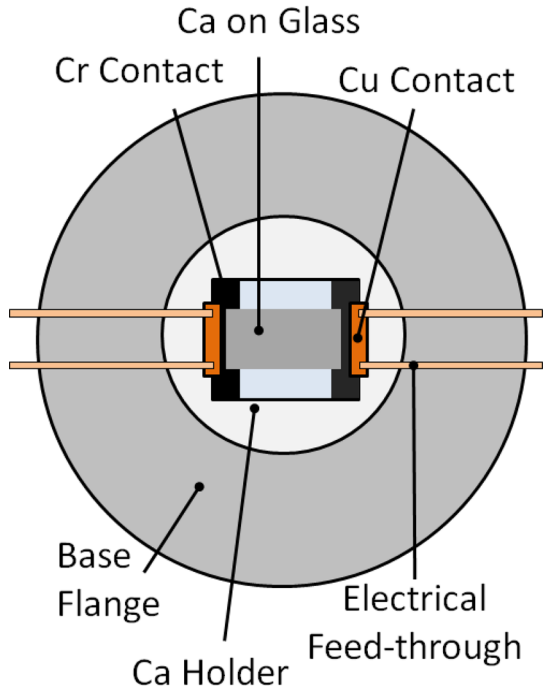

Figure 1. Schematic top-down view of the calcium film sensor.

The base flange was made from a standard $4^1/_2$ in. CF viewport and was fitted with a holder for the Ca film sensor. The viewport allowed the Ca film to be visually monitored with a USB microscope. The holder was made from stainless steel. Contact insulators on the holder were made from Macor. These insulators prevented the electrical contacts from shorting to the

dx.doi.org/10.1021/jp4043057 | J. Phys. Chem. A XXXX, XXX, XXX−XXX

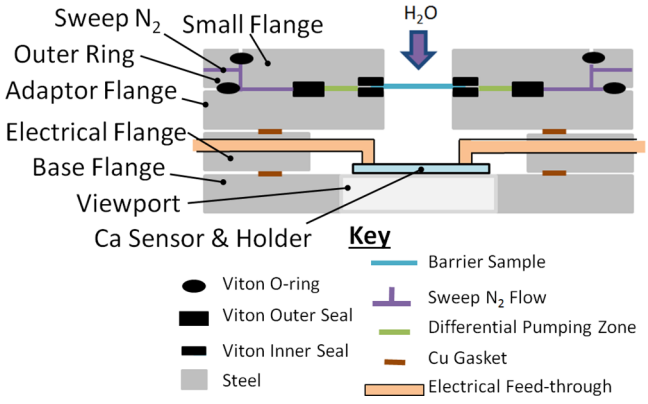

Figure 2. Schematic cross-sectional view of the calcium film sensor on the base flange in the test apparatus.

apparatus body. The base flange was baked for at least 24 h at 120 °C under 1 Torr of Ar or N_2 prior to each use to ensure consistent results.

The electrical flange was made from a double sided $4^1/_2$ in. CF flange containing copper electrical feedthroughs. Copper connections on the interior of the feedthrough provided electrical contact to the Ca film sensor. Solder connections were not used to avoid thermocouple junctions. The copper connection utilized a copper mesh that provided flexibility in assembly. The copper mesh was attached to the copper electrical feedthrough and copper contact close to the Ca film using crimp connectors. The copper leads on the exterior of the electrical feedthrough were terminated in gold-plated dual banana plugs that were plugged into the ammeter.

The adapter flange was designed with two concentric seal regions around the edge of the polymer sample. Figure 3 shows

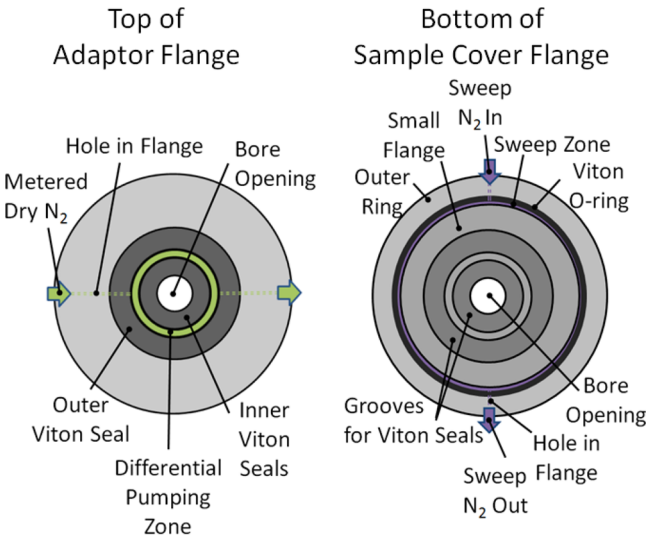

Figure 3. Schematic of the top of the adaptor flange and the bottom of the sample cover flange.

this sealing design that prevents H_2O or O_2 from entering the Ca test apparatus. The two inner Viton seals sandwich the polymer sample while the outer Viton seal provides a differential pumping region between the inner and outer Viton seals. The two inner seals were half the thickness of the single outer seal such that minimal mechanical strain was exerted on the polymer sample. Even a relatively small mechanical strain on the polymer substrate could result in failure of the Al_2O_3 ALD gas diffusion barrier due to cracking.

The Viton seals were baked for at least 72 h before use to remove absorbed water.[26,27] Figure 3 shows two ports at 180° that were machined into the adaptor flange to allow pumping of the differential region between the Viton seals. A metered dry N_2 line was attached to one port and the other port was connected to pumping. The differential pumping zone was purged with a constant filtered flow of dry N_2 from a liquid nitrogen tank for the duration of the test. The N_2 pressure within the differential pumping zone was maintained between 1 and 2 Torr.

The sample cover flange consisted of the small flange that sat inside the outer ring. The small flange was machined with grooves for the inner and outer Viton seals shown in Figure 3. The small flange seated snugly inside the outer ring and was sealed to the outer ring using a Viton O-ring seal. This allowed for substitution of the small flange with a flange of the same size but without a center bore opening. This small flange with no bore opening was used as a control lid to determine the baseline of the experiment.

The outer ring was machined to provide a space for dry N_2 to flow when the outer ring sealed around the small flange. The outer ring had inlet and outlet ports mounted 180° apart. A dry N_2 line called the "sweep N_2" was attached to the inlet. The outlet port was left open to the humidity chamber. The machined gap between the small flange and outer ring was flushed with "sweep N_2" above atmospheric pressure for the duration of the test. This gap is called the "sweep zone". The top surface of the adaptor flange was sealed to the outer ring using a Viton O-ring that was positioned just outside the "sweep zone".

C. Humidity Chamber and Electrical Conductance Measurements. The environmental chamber (ESPEC BTL-400) utilized a Watlow F4 controller that was linked to LabView using an RS-232 (Modbus-RTU) connection. A custom LabView program was used to record the sample conductance five times at 1 min intervals for each sample. The measurements were averaged to attenuate any electrical noise present in the signal. The same program recorded the temperature and humidity reported by the Watlow controller.

A four-wire resistance measurement was used to increase accuracy in the determination of the electrical conductance. Using four-wire resistance helps to minimize the lead resistance and cancels minor differences in lead length and crimped connections. The electrical conductance of the Ca film was monitored with a Keithley 2700/7700 mainframe and multiplexer combination inside a grounded Faraday cage. To further reduce electrical noise, the meter and computer were powered using a line power conditioner. This instrumentation allowed multiple samples to be run in parallel through the entire experiment.

3. MODELING OF H_2O DIFFUSIVE FLUX

The concentration of H_2O in the Ca test apparatus in the absence of the PEN polymer was modeled using a one-dimensional form of Fick's second law:[28]

$$\frac{\partial C_w[t,z]}{\partial t} = D_{aw}\frac{\partial^2 C_w[t,z]}{\partial z^2} \quad (1)$$

This equation was solved with the boundary conditions $C_w[t>0,0] = C_0$, $C_w[t>0,h] = 0$, and the initial condition

dx.doi.org/10.1021/jp4043057 | J. Phys. Chem. A XXXX, XXX, XXX−XXX

$C_w[0,z] = 0$. In this equation, C_w is the concentration of water, D_{aw} is the diffusivity of water in air, and $h = 6.2$ cm is the distance from the top face of the sample cover flange to the surface of the Ca film.

The boundary condition $C_w[t>0,h] = 0$ assumes the instantaneous reaction of every H_2O molecule that collides with the calcium surface. In addition, there is no radial dependence of the H_2O concentration. There is also a uniform temperature in the Ca test apparatus. The solution for $C_w[t,z]$ with these boundary conditions takes the form of a Fourier series:[29]

$$C_w[t,z] = C_w^{ss} + \sum_{\infty}^{n=1} A_n e^{-\lambda_n^2 D_{aw} t} \sin[\lambda_n z] \quad (2)$$

where

$$\lambda_n = \frac{n\pi}{h} \quad (3)$$

$$A_n = \int_0^h \frac{2}{h}(C_w[0,z] - C_w^{ss}) \sin[\lambda_n z]\, dz \quad (4)$$

$$C_w^{ss} = C_0\left(1 - \frac{z}{h}\right) \quad (5)$$

These equations also yield the H_2O flux onto the calcium surface as

$$J_h[t] = -D_{aw}\left.\frac{\partial C_w[t,z]}{\partial z}\right|_{z=h} \quad (6)$$

Under the assumption that all the H_2O molecules that collide with the Ca film react with the Ca film, the total moles of water reacted per unit area of calcium is

$$N[t] = \int_0^t J_h[t']\, dt' \quad (7)$$

Results obtained using this model included only the first 20 terms of the Fourier series given in eq 2.

4. RESULTS AND DISCUSSION

The conductance of the Ca sensor film decreases as the Ca film is oxidized by O_2 or H_2O exposure. Because the humidity chamber is purged with N_2, all Ca oxidation will be attributed to water. H_2O has also been shown to be much more effective at oxidizing Ca than O_2.[18,30] A conductance curve for a PEN polymer coated with an Al_2O_3 ALD barrier with a thickness of 25 nm is shown in Figure 4. These results were obtained using 70 °C and 80% relative humidity (RH). The conductance curve shows a characteristic form. The conductance is initially very flat versus H_2O exposure time. The conductance then drops rapidly at later H_2O exposure times. The conductance reaches zero at ~280 h with an Al_2O_3 ALD gas diffusion barrier on the PEN polymer.

Initial conductance that does not change for a certain H_2O exposure time is often interpreted as a "lag time".[31] This lag time could be caused by a long tortuous path for H_2O molecules through the barrier film. The lag time may also be explained as a "reservoir effect" where H_2O must fill up the polymer prior to leaving the polymer.[32] In addition, the lag time may be caused by resistance in series with the Ca film that is larger than the Ca film itself.[33] The Ca film then does not influence the resistance measurements until later stages of Ca film oxidation. The transition to the "fall off" region may also be

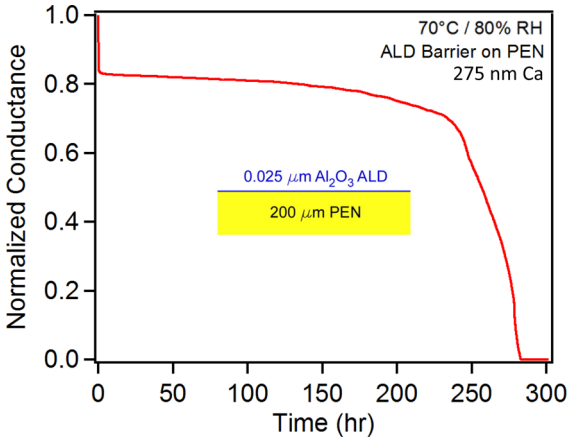

Figure 4. Normalized conductance versus time for a 0.025 μm Al_2O_3 ALD barrier on a PEN polymer with a thickness of 200 μm. The Ca film thickness was 275 nm, and the experimental conditions were 70 °C and 80% RH.

caused by H_2O dissolution of the Al_2O_3 barrier.[34] To determine whether the negligible change in the initial conductance is related to the Al_2O_3 ALD barrier or the PEN polymer, a series of experiments were performed to examine the behavior of the PEN polymer by itself.

The conductance versus time for a bare PEN polymer at 70 °C/40% RH is shown in Figure 5. The functional form of the

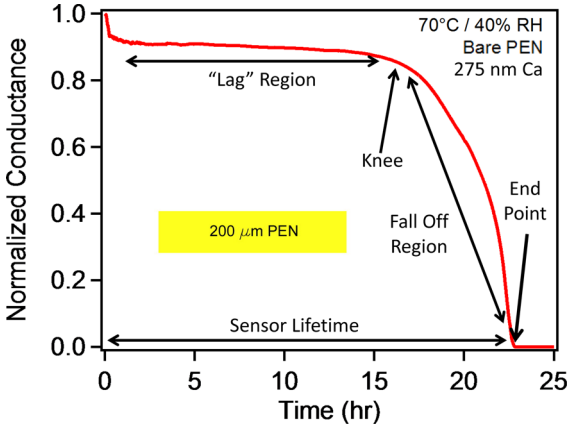

Figure 5. Normalized conductance versus time for a bare PEN polymer with a thickness of 200 μm. The Ca film thickness was 275 nm, and the experimental conditions were 70 °C and 40% RH.

conductance versus H_2O exposure time in Figure 5 is very similar to the results in Figure 4. However, the time required for the conductance to reach zero is much shorter. The conductance reaches zero in ~23 h in Figure 5 for the PEN polymer compared with ~280 h in Figure 4 for the PEN polymer coated with the Al_2O_3 ALD barrier. The Ca film thickness was constant at ~275 nm for the results in Figures 4 and 5.

Figure 5 is also used to define the terms for the different parts of the Ca film conductance versus H_2O exposure time curve. The initial conductance is nearly constant in the "lag region". The lag region occurs until the "knee". After the knee, the decrease of the conductance is the "fall off region". The point at which the conductance reaches zero is the "end point". From $t = 0$ to the end point when the conductance is zero is the "sensor lifetime".

dx.doi.org/10.1021/jp4043057 | J. Phys. Chem. A XXXX, XXX, XXX−XXX

Additional conductance measurements were performed to determine the sensor lifetime as a function of relative humidity at 70 °C. These experiments were again performed for bare PEN polymer substrates. The results at 25% RH and 60% RH are shown in Figure 6. The effect of the H_2O % RH on the Ca

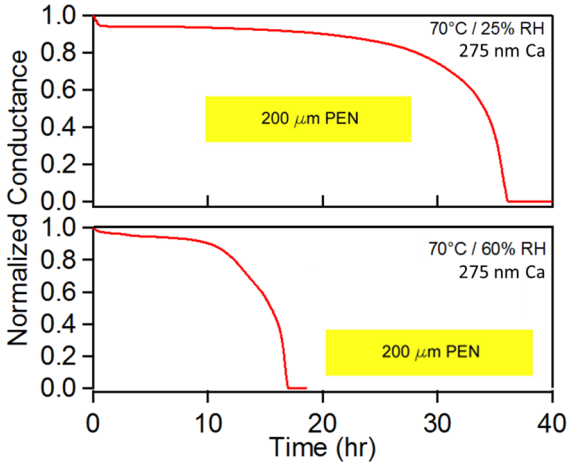

Figure 6. Normalized conductance versus time for a bare PEN polymer with a thickness of 200 μm at 70 °C/25% RH and 70 °C/60% RH. The Ca film thickness was 275 nm.

film lifetime is significant. The sensor lifetime for 25% RH is ~36 h. The sensor lifetime for 60% RH is ~18 h. The sensor lifetime is approximately inversely related to the % RH.

Figure 7 shows the dependence of the sensor lifetime versus 1/flux at 70 °C. The Ca film lifetime is linearly dependent on

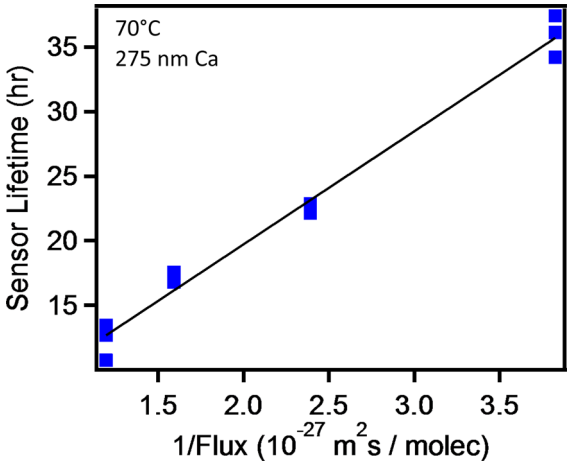

Figure 7. Sensor lifetime versus 1/flux at 70 °C for a bare PEN polymer with a thickness of 200 μm. The Ca film thickness was 275 nm.

1/flux. The sensor lifetime is shorter for the higher H_2O vapor pressures at 70 °C. This dependence is consistent with a simple mechanism where each H_2O collision with the PEN polymer has a certain probability of transmitting H_2O through the polymer. A schematic of the interaction and transmission of H_2O through a polymer is shown in Figure 8.

The assumed mechanism displayed in Figure 8 is a multistep process. The incident water molecule first adsorbs and resides on the polymer surface prior to either desorbing from the polymer or absorbing into the polymer. After absorbing and

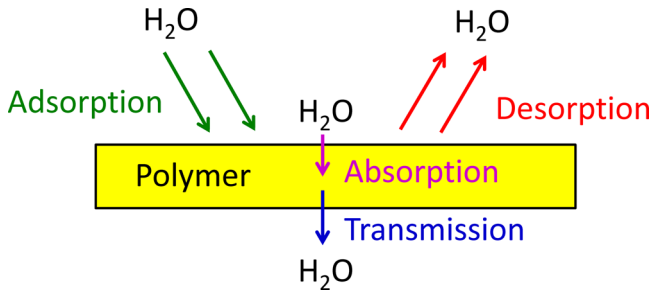

Figure 8. Schematic of the H_2O processes on the polymer including adsorption, desorption, absorption, and transmission.

subsequently diffusing through the polymer, the H_2O molecule can desorb from the other side of the polymer. The H_2O molecules that desorb from the other side of the polymer are the transmitted H_2O molecules. These H_2O molecules enter the Ca test apparatus and oxidize the Ca film.

The transmission coefficient for H_2O through the PEN polymer is the number of H_2O molecules that are transmitted through the PEN polymer divided by the number of H_2O of molecules that are incident on the PEN polymer surface. The transmission coefficient is calculated by

$$\Gamma = \frac{N}{J_0 t_f} \tag{8}$$

N is the number of H_2O molecules that are needed to oxidize the Ca film to form $Ca(OH)_2$, J_0 is the incident H_2O flux on the PEN polymer, and t_f is the sensor lifetime, i.e., the time required for the normalized conductance to reach zero. The transmission coefficient and the incident H_2O flux define the water vapor transmission rate (WVTR) according to

$$\mathrm{WVTR} = J_0\Gamma \tag{9}$$

This WVTR has units of molecules/(m^2 h) and can be easily converted to the units of g/(m^2 day) more commonly employed for the WVTR. For the determination of the transmission coefficient, the H_2O flux onto the polymer surface was derived from kinetic gas theory:

$$J_0 = P/\sqrt{2\pi mkT} \tag{10}$$

P is the partial pressure of water, m is the mass of a water molecule, k is the Boltzmann constant, and T is the temperature.

For a given calcium film thickness, h, the number of water molecules needed to fully oxidize a unit area of the calcium film with 20 at. % oxygen as determined by XPS analysis is given by

$$N = \frac{h\rho w_{Ca} q n N_A}{m_{Ca}} \tag{11}$$

In this equation, the density of the Ca film was derived by assuming that the Ca film with 20 atom % oxygen is composed of bulk Ca and bulk CaO. If all the oxygen is present as CaO, then a simple "rule of mixtures" calculation yields a density of $\rho \cong 1.86$ g/cm^3. $w_{Ca} \cong 0.91$ is the mass fraction of calcium in the film, $q \cong 0.825$ is the fraction of Ca atoms available to be oxidized, $n = 2$ is the stoichiometric ratio for H_2O:Ca for the calcium oxidation reaction to form $Ca(OH)_2$, N_A is Avogadro's number, and m_{Ca} is the atomic mass of calcium.

For the H_2O vapor transmission measurements at 70 °C, eq 10 can be simplified to $J_0 \cong 3.78 \times 10^{28}$ molecules/(m^2 h) × %

dx.doi.org/10.1021/jp4043057 | J. Phys. Chem. A XXXX, XXX, XXX−XXX

RH. Equation 11 yields $N \cong 1.16 \times 10^{22}$ molecules/m^2 for a calcium thickness of 275 nm. Therefore, the transmission coefficient at these conditions is given by

$$\Gamma \cong \frac{3.07 \times 10^{-7}}{\%\ \mathrm{RH} \times t_f} \quad (12)$$

where t_f is in units of hours. These definitions can be used to determine transmission coefficients and WVTRs for the data in Figures 4−7 on the basis of the time required to oxidize the Ca film. This sensor lifetime is based on the end point for the normalized conductance of the Ca film. The transmission coefficient and WVTR values are given in Table 1.

Table 1. Transmission Coefficients and WVTR Values for H_2O Vapor Transmission through the PEN Polymer at 70°C and different H_2O Relative Humidities[a]

condition	RH (%)	t_f (h)	J_0 [10^{29} molecules/(m^2·h)]	Γ (10^{-11})	WVTR [g/(m^2·day)]
ALD on PEN	80	280	30	1.4	0.030
bare PEN	80	13	30	30	0.65
bare PEN	60	17	23	30	0.49
bare PEN	40	23	15	33	0.36
bare PEN	25	36	9.5	34	0.23

[a]The H_2O fluxes corresponding to the H_2O relative humidities and the times required for the normalized conductance to reach zero are also given.

Additional experiments examined the temperature dependence of the Ca film lifetime at constant H_2O flux. A constant flux onto the polymer surface was maintained by changing both temperature and humidity within the environmental chamber. Figure 9 shows that the sensor lifetime versus temperature

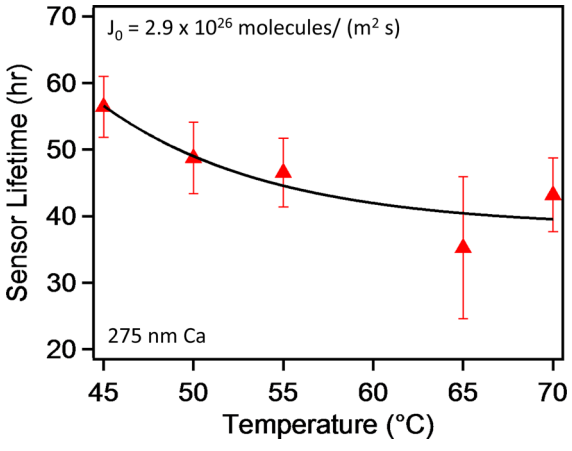

Figure 9. Sensor lifetime for a Ca film thickness of 275 nm with a H_2O flux of 2.9×10^{16} molecules/(m^2 s) on a bare PEN polymer with a thickness of 200 μm at various temperatures.

decreased only slightly with temperature at a fixed flux of $J_0 = 2.9 \times 10^{26}$ molecules/(m^2 s). The error bars represent one standard deviation for the three samples that were tested at each temperature.

The temperature dependent sensor lifetime data in Figure 9 was analyzed assuming Arrhenius dependence. The plot of ln (1/sensor lifetime) versus $1/T$ is displayed in Figure 10. This plot yields an activation energy of E = 12.4 kJ/mol. This activation energy results from the temperature dependence of

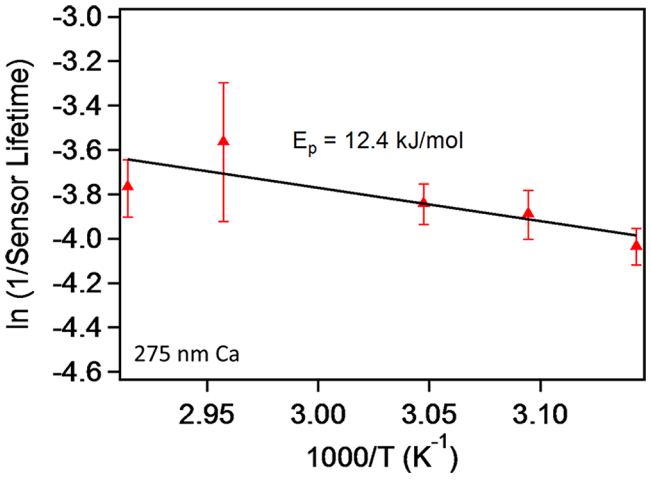

Figure 10. Arrhenius plot of the sensor lifetimes versus temperature in Figure 9.

the H_2O sticking coefficient, the barrier for H_2O desorption from the polymer surface, and the barrier for H_2O vapor transmission through the PEN polymer. H_2O desorption will lower the H_2O residence time on the polymer surface and decrease the number of H_2O molecules entering the polymer. The effect of increased H_2O desorption alone would be expected to decrease the transmission coefficient and increase the sensor lifetime.

Figure 9 shows that the sensor lifetime decreases at higher temperatures. This decreasing sensor lifetime is consistent with more H_2O molecules transmitted through the PEN polymer at higher temperature. This behavior argues that the activation barrier for H_2O vapor transmission through the polymer is larger than the activation barrier for H_2O desorption from the polymer surface. The actual barrier for H_2O vapor transmission through the polymer is expected to be higher than E = 12.4 kJ/mol because H_2O desorption lowers the H_2O vapor transmission rate at higher temperatures.

The interpretation of the "lag time" is still uncertain. The sensor lifetime is inversely dependent on the H_2O flux at constant temperature and the sensor lifetime includes the lag time. To check whether a reservoir effect causes the lag time, the sensor lifetime was measured for both dry and water-saturated PEN polymers at 70 °C. Figure 11 shows the results for a dry polymer and a polymer saturated with H_2O at 60% RH. The sensor lifetime showed no observable difference between a dry or H_2O saturated PEN polymer.

The sensor lifetimes were measured versus % RH at 70 °C. The relative humidity was varied between the lower and upper limits of the humidity chamber from 25% to 80% RH. Figure 12 reveals that there is no difference between dry or H_2O-saturated PEN polymers. Estimates of the transmission coefficient and water vapor transmission rate for these conditions yield values of $\Gamma = 3.0 \times 10^{-10}$ and WVTR = 0.49 g/(m^2 day) for the saturated polymer at 60% RH, and $\Gamma = 2.7 \times 10^{-10}$ and WVTR = 0.44 g/(m^2 day) for the dry polymer at 60% RH. These results indicate that there is no H_2O reservoir in the PEN polymer. The lag region in the plots of conductance versus time cannot be attributed to a H_2O reservoir effect.

Because the lag region cannot be attributed to the PEN polymer, additional experiments were performed by measuring the conductance versus H_2O exposure time with *no polymer film* between the H_2O flux and the Ca film. The polymer was

dx.doi.org/10.1021/jp4043057 | J. Phys. Chem. A XXXX, XXX, XXX−XXX

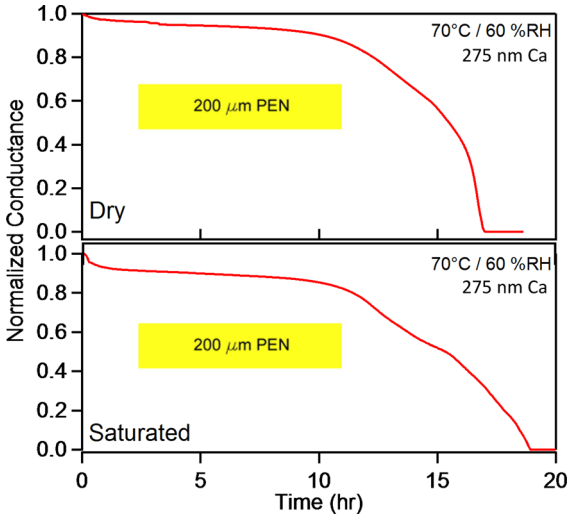

Figure 11. Normalized conductance versus time for a dry and saturated PEN polymer with a thickness of 200 μm. The Ca film thickness was 275 nm and the experimental conditions were 70 °C and 60% RH.

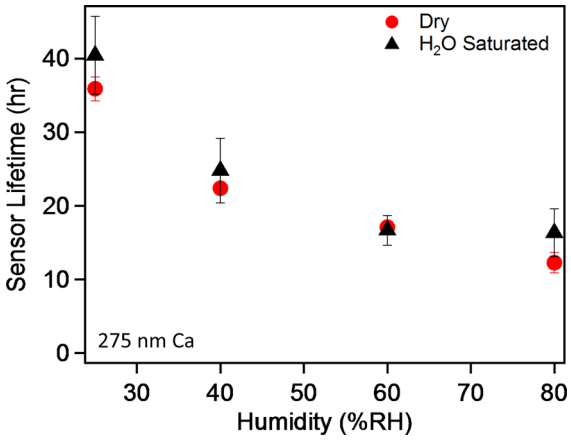

Figure 12. Sensor lifetimes versus % RH at 70 °C for dry and saturated PEN polymer with a thickness of 200 μm. The Ca film thickness was 275 nm.

removed from the test apparatus before measuring the conductance. Figure 13 shows the experimental conductance versus time at 70 °C and 25% RH. The low humidity was chosen to extend the life of the Ca film for as long as possible. In addition, the Ca film thickness was increased to ~550 nm by doubling the Ca deposition time to ~20 min. This larger Ca film thickness was confirmed by FIB-SEM measurements.

The experimental conductance versus time shown in Figure 13 again has the same functional form as the previous curves shown in Figures 4–6 and 11. However, the sensor lifetime is now only ~9 min. This experiment was conducted six times. Each experiment showed the same response with the same functional form for the conductance versus time and sensor lifetimes between 7 and 9 min.

The results for the sensor lifetime with no polymer film were modeled using one-dimensional Fickian diffusion. These calculations determined whether H_2O diffusion into the Ca test apparatus could account for the ~8 min lag region. The Ca film was assumed to oxidize linearly versus H_2O exposure. The normalized conductance was assumed to be proportional to the unreacted Ca film thickness. These calculations assumed

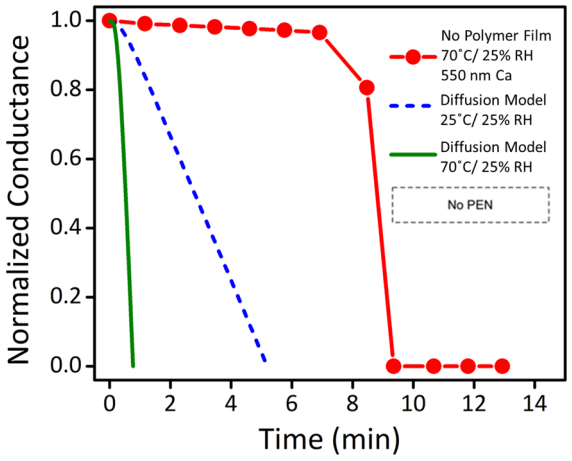

Figure 13. Normalized conductance versus time at 70 °C/25% RH for a Ca film with a thickness of 550 nm with no PEN polymer. Calculations of the predicted conductance based on a diffusion model are shown for comparison at 70 °C/25% RH and 25 °C/25% RH.

oxidation of the Ca film to form $Ca(OH)_2$ and an initial Ca film thickness of 550 nm.

The predicted normalized conductances shown in Figure 13 were generated for 70 °C/25% RH and 25 °C/25% RH. The predictions at 25 °C/25% RH were performed to establish an upper limit on the predictions at 25% RH. For 70 °C/25% RH, C_0 = 3.10 μmol/cm^3 and D_{aw} = 19.2 cm^2/min.[35,36] For 25 °C/25% RH, C_0 = 0.32 μmol/cm^3 and D_{aw} = 15.0 cm^2/min.[35,36] The difference between the predictions at 25 and 70 °C results from the higher absolute H_2O concentration for 25% RH at 70 °C.

The model predicts a sensor lifetime of 0.77 min at 70 °C/25% RH. This prediction is an order of magnitude less than the experimental value at 70 °C/25% RH. The model predicts a sensor lifetime of 5.19 min at 25 °C/25% RH. This prediction is 42% less than the experimental value at 70 °C/25% RH. These predictions reveal that H_2O diffusion into the Ca test apparatus cannot be the sole cause of the lag in the Ca film sensor response. These results suggest that the lag in the Ca film response must be caused by the oxidation of the Ca film itself.

The experimental Ca film conductance versus H_2O exposure time shows the same functional form whether there is no polymer, a bare PEN polymer, or an ALD barrier on the PEN polymer to restrict the H_2O flux. Only the time scale changes between the different experiments. The results for the bare PEN polymer and the ALD barrier on the PEN polymer could be explained by a resistance in series with the Ca film that dominates the measurements until the Ca film resistance increases at later stages of Ca film oxidation.[33]

To measure the resistance in series with the Ca film, the resistance was determined for different Ca film thicknesses using four-wire resistance measurements performed inside the glovebox with a Cr film thickness of ~540 nm. Resistance measurements were obtained for Ca film thicknesses of 270, 410, and 570 nm. These thicknesses were determined using FIB/SEM analysis on reference samples. The slope of the plot of resistance versus 1/thickness was then employed to determine the film resistivity using $R = \rho l/A$ where R is resistance, ρ is resistivity, l is the length of the film, and A is the cross-sectional area of the film. A resistivity of $\rho = 1.34 \times 10^{-4}$ Ω cm was obtained for these Ca films containing 20 at. % O.

dx.doi.org/10.1021/jp4043057 | J. Phys. Chem. A XXXX, XXX, XXX–XXX

The *y*-intercept of the plot of resistance versus 1/thickness yielded a resistance of 0.23 Ω. This is the resistance in series with the Ca film. This series resistance is attributed to the Cu/Cr contact resistances, the Cr film resistances, and the Cr film/Ca contact resistances. This series resistance is negligible compared with the measured resistance of ~10 Ω for the initial Ca film samples. These measurements argue that resistance in series with the Ca film does not dominate the resistance at the initial stages of Ca film oxidation. The nearly constant Ca film conductance during the initial H_2O exposure is attributed to the nonlinear oxidation kinetics of the Ca film.

Although the initial oxidation kinetics of the Ca film display nonlinearity, the time required for the normalized conductance to reach zero is inversely dependent on the H_2O flux. This behavior indicates that the Ca film may require a threshold number of H_2O molecules to initiate Ca film oxidation. After reaching this threshold, the Ca film may react readily with all the H_2O molecules. This explanation could explain the observation that the sensor lifetime is inversely dependent on the H_2O flux.

The nonlinear oxidation kinetics of the Ca film may not be surprising given the very inhomogeneous nature of Ca film oxidation that has been revealed by recent atomic force microscope (AFM) studies.[33,37] The AFM investigations showed that H_2O exposure leads to considerable film roughening. Nonlinear oxidation kinetics were also reported by previous studies of Ca film oxidation by H_2O.[18,19,38] The Ca film oxidation kinetics varied versus temperature and H_2O exposure time. Deviations from linearity were especially apparent during the initial stages of Ca film oxidation.

The nonlinear oxidation kinetics of the Ca film will affect the WVTR values determined using the Ca test. The Ca test assumes a linear oxidation of the Ca film versus H_2O exposure. This linear oxidation is then assumed to produce a linear decrease in the conductance of the Ca film. The rate of the conductance change versus time yields a WVTR value.[17] In contrast, a nonlinear decrease in the conductance of the Ca film is observed as exemplified by the results shown in Figure 4. The conductance versus time in Figure 4 can be analyzed to determine how the nonlinear oxidation kinetics affect the derived WVTR values.

At early times during the H_2O exposure, the change in the conductance versus time is negligible. This region was defined as the "lag region" in Figure 5. The "lag region" of Figure 4 yields a WVTR value of ~0.002 g/(m^2 day). At later times during the H_2O exposure, the change in the conductance versus time is substantial. This region was defined as the "fall off" region in Figure 5. The "fall off" region of Figure 4 yields a WVTR value of ~0.40 g/(m^2 day). In contrast, end point analysis using the "sensor lifetime" was employed to calculate the WVTR values given in Table 1. Using end point analysis, Figure 4 yields a WVTR value of ~0.03 g/(m^2 day). End point analysis is equivalent to assuming a linear decrease in conductance of the Ca film.

The WVTR values obtained from Figure 4 vary from ~0.002 to ~0.40 g/(m^2 day). The WVTR value derived from the end point analysis is ~0.03 g/(m^2 day). This WVTR is in the middle between the low WVTR value obtained from the "lag region" and the high WVTR value obtained from the "fall off" region. The WVTR value derived from the end point analysis is the most reliable because this value does not depend on the specific oxidation kinetics of the Ca film. The only assumption of the end point analysis is that all the H_2O molecules will eventually react with the Ca film. Future applications of the Ca test to determine WVTR values should be performed until the Ca film is completely oxidized to remove the uncertainty from the nonlinear oxidation kinetics of the Ca film.

5. CONCLUSIONS

H_2O vapor transmission through PEN polymer with a thickness of 200 μm was measured using the electrical Ca test. The H_2O vapor transmission rate was determined as a function of the H_2O flux, temperature, and saturation of the PEN polymer with H_2O. Using the time required for the normalized conductance of the Ca film to reach zero, the measurements revealed that the H_2O vapor transmission rate was dependent on the H_2O flux and only weakly dependent on temperature at constant H_2O flux. The transmission coefficient for H_2O through the PEN polymer was $\Gamma \sim 3.2 \times 10^{-10}$ at 70 °C. The WVTR at 70 °C/80% RH corresponding to this transmission rate was 0.65 g/(m^2 day). An activation barrier of E = 12.4 kJ/mol was obtained from the temperature dependence of the H_2O vapor transmission rate through PEN polymer at constant H_2O flux. The H_2O vapor transmission rates for initially dry or H_2O-saturated PEN polymer substrates at various temperatures were nearly identical. These results indicate that there is no reservoir effect for H_2O in the PEN polymer.

The Ca film conductance did not decrease linearly versus H_2O exposure. The initial Ca film conductance was nearly constant during H_2O exposure. The conductance then decreased abruptly after longer H_2O exposure times. The nearly constant initial Ca film conductance versus H_2O exposure could not be explained by a resistance in series with the Ca film. In addition, the results for Ca film oxidation in the absence of the PEN polymer are not consistent with linear oxidation kinetics. Nonlinear initial oxidation kinetics of the Ca film are required to explain the nonlinear dependence of the Ca film conductance versus H_2O exposure.

AUTHOR INFORMATION

Corresponding Author

*E-mail: steven.george@colorado.edu.

Notes

The authors declare no competing financial interest.

ACKNOWLEDGMENTS

This work was supported by the Defense Advanced Research Projects Agency (DARPA) under Contract Numbers N10PC20168 and D11PC20172, through SBIR Phase I and II programs led by Dr. Markus Groner at ALD NanoSolutions, Inc. The authors acknowledge useful discussions with Uwe Schröder and Hannes Klumbies at the University of Dresden. The authors also thank Andrew S. Cavanagh for XPS analysis of the Ca films.

REFERENCES

(1) Wijmans, J. G.; Baker, R. W. The Solution-Diffusion Model - A Review. *J. Membr. Sci.* **1995**, *107*, 1−21.

(2) Allen, S. M.; Fujii, M.; Stannett, V.; Hopfenberg, H. B.; Williams, J. L. Barrier Properties of Polyacrylonitrile. *J. Membr. Sci.* **1977**, *2*, 153−164.

(3) Barrie, J. A. In *Diffusion in Polymers*; Crank, J., Park, G. S., Eds.; Academic Press: New York, 1968.

(4) Barrie, J. A.; Platt, B. The Diffusion and Clustering of Water Vapour in Polymers. *Polymer* **1963**, *4*, 303−313.

(5) Chen, G. Q.; Scholes, C. A.; Qiao, G. G.; Kentish, S. E. Water Vapor Permeation in Polyimide Membranes. *J. Membr. Sci.* **2011**, *379*, 479−487.
(6) Debeaufort, F.; Voilley, A.; Meares, P. Water-Vapor Permeability and Diffusivity through Methylcellulose Edible Films. *J. Membr. Sci.* **1994**, *91*, 125−133.
(7) Despond, S.; Espuche, E.; Domard, A. Water Sorption and Permeation in Chitosan Films: Relation Between Gas Permeability and Relative Humidity. *J. Polym. Sci. Polym. Phys.* **2001**, *39*, 3114−3127.
(8) Schult, K. A.; Paul, D. R. Water Sorption and Transport in a Series of Polysulfones. *J. Polym. Sci. Polym. Phys.* **1996**, *34*, 2805−2817.
(9) Zhang, Z. B.; Britt, I. J.; Tung, M. A. Permeation of Oxygen and Water Vapor Through EVOH Films As Influenced by Relative Humidity. *J. Appl. Polym. Sci.* **2001**, *82*, 1866−1872.
(10) Stern, S. A. Barrer Permeability Unit. *J. Polym. Sci. A2* **1968**, *6*, 1933−1934.
(11) MacDonald, W. A. Engineered Films for Display Technologies. *J. Mater. Chem.* **2004**, *14*, 4−10.
(12) Carcia, P. F.; McLean, R. S.; Groner, M. D.; Dameron, A. A.; George, S. M. Gas Diffusion Ultrabarriers on Polymer Substrates Using Al_2O_3 Atomic Layer Deposition and SiN Plasma-Enhanced Chemical Vapor Deposition. *J. Appl. Phys.* **2009**, *106*, 023533.
(13) Carcia, P. F.; McLean, R. S.; Reilly, M. H.; Groner, M. D.; George, S. M. Ca Test of Al_2O_3 Gas Diffusion Barriers Grown by Atomic Layer Deposition on Polymers. *Appl. Phys. Lett.* **2006**, *89*, 031915.
(14) Lewis, J. S.; Weaver, M. S. Thin-Film Permeation-Barrier Technology for Flexible Organic Light-Emitting Devices. *IEEE J. Sel. Top. Quant. Elect.* **2004**, *10*, 45−57.
(15) Kumar, R. S.; Auch, M.; Ou, E.; Ewald, G.; Jin, C. S. Low Moisture Permeation Measurement through Polymer Substrates for Organic Light Emitting Devices. *Thin Solid Films* **2002**, *417*, 120−126.
(16) Nisato, G.; Bouten, P. C. P.; Slikkerveer, P. J.; Bennett, W. D.; Graff, G. L.; Rutherford, N.; Wiese, L. Evaluating Higher Performance Diffusion Barriers: The Calcium Test. *Proc. Asia Display/IDW '01* **2001**, 1435.
(17) Paetzold, R.; Winnacker, A.; Henseler, D.; Cesari, V.; Heuser, K. Permeation Rate Measurements by Electrical Analysis of Calcium Corrosion. *Rev. Sci. Instrum.* **2003**, *74*, 5147−5150.
(18) Gregg, S. J.; Jepson, W. B. Oxidation of Calcium in Moist Oxygen. *J. Chem. Soc.* **1961**, 884−888.
(19) Svec, H. J.; Apel, C. Metal-Water Reactions. 4. Kinetics of the Reaction Between Calcium and Water Vapor. *J. Electrochem. Soc.* **1957**, *104*, 346−349.
(20) Chen, T. N.; Wuu, D. S.; Wu, C. C.; Chiang, C. C.; Chen, Y. P.; Horng, R. H. Improvements of Permeation Barrier Coatings Using Encapsulated Parylene Interlayers for Flexible Electronic Applications. *Plasma Process. Polym.* **2007**, *4*, 180−185.
(21) Choi, J. H.; Kim, Y. M.; Park, Y. W.; Huh, J. W.; Ju, B. K.; Kim, I. S.; Hwang, H. N. Evaluation of Gas Permeation Barrier Properties Using Electrical Measurements of Calcium Degradation. *Rev. Sci. Instrum.* **2007**, *78*, 064701.
(22) Kim, T. W.; Yan, M.; Erlat, G.; McConnelee, P. A.; Pellow, M.; Deluca, J.; Feist, T. P.; Duggal, A. R.; Schaepkens, M. Transparent Hybrid Inorganic/Organic Barrier Coatings for Plastic Organic Light-Emitting Diode Substrates. *J. Vac. Sci. Technol. A* **2005**, *23*, 971−977.
(23) Meyer, J.; Gorrn, P.; Bertram, F.; Hamwi, S.; Winkler, T.; Johannes, H. H.; Weimann, T.; Hinze, P.; Riedl, T.; Kowalsky, W. Al_2O_3/ZrO_2 Nanolaminates as Ultrahigh Gas-Diffusion Barriers-A Strategy for Reliable Encapsulation of Organic Electronics. *Adv. Mater.* **2009**, *21*, 1845−1849.
(24) Reese, M. O.; Dameron, A. A.; Kempe, M. D. Quantitative Calcium Resistivity Based Method for Accurate and Scalable Water Vapor Transmission Rate Measurement *Rev. Sci. Instrum.* **2011**, *82*,
(25) Bertrand, J. A.; George, S. M. Evaluating Al_2O_3 Gas Diffusion Barriers Grown Directly on Ca Films Using Atomic Layer Deposition Techniques *J. Vac. Sci. Technol. A* **2013**, *31*,
(26) Crawley, D. J.; Decserna., L. Degassing Characteristics of Some O-Ring Materials. *Vacuum* **1964**, *14*, 7−9.
(27) De Csernatony, L. The Properties of Viton A Elastomers. II. Influence of Permeation, Diffusion and Solubility of Gases on Gas Emission Rate from an O-Ring Used as an Atmospheric Seal or High Vacuum Immersed. *Vacuum* **1966**, *16*, 129−134.
(28) Bird, R.; Stewart, W.; Lightfoot, E. *Transport Phenomena*; John Wiley & Sons: New York, 2002.
(29) Asmar, N. H. *Partial Differential Equations with Fourier Series and Boundary Value Problems*: Pearson/Prentice Hall: Englewood Cliffs, NJ, 2005.
(30) Cros, S.; Firon, M.; Lenfant, S.; Trouslard, P.; Beck, L. Study of Thin Calcium Electrode Degradation by Ion Beam Analysis. *Nucl. Instrum. Methods Phys. Res., Sect. B* **2006**, *251*, 257−260.
(31) Graff, G. L.; Williford, R. E.; Burrows, P. E. Mechanisms of Vapor Permeation Through Multilayer Barrier Films: Lag Time versus Equilibrium Permeation. *J. Appl. Phys.* **2004**, *96*, 1840−1849.
(32) van der Wel, G. K.; Adan, O. C. G. Moisture in Organic Coatings - A Review. *Prog. Org. Coat.* **1999**, *37*, 1−14.
(33) Schubert, S.; Klumbies, H.; Muller-Meskamp, L.; Leo, K. Electrical Calcium Test for Moisture Barrier Evaluation for Organic Devices. *Rev. Sci. Instrum.* **2011**, *82*, 094101.
(34) Dameron, A. A.; Davidson, S. D.; Burton, B. B.; Carcia, P. F.; McLean, R. S.; George, S. M. Gas Diffusion Barriers on Polymers Using Multilayers Fabricated by Al_2O_3 and Rapid SiO_2 Atomic Layer Deposition. *J. Phys. Chem. C* **2008**, *112*, 4573−4580.
(35) Bolz, R. E.; Tuve, G. L. *CRC Handbook of Tables for Applied Engineering*; CRC Press: New York, 1976.
(36) Hirschfelder, J. O.; Curtiss, C. F.; Bird, R. B. *Molecular Theory of Gases and Liquids*; John Wiley & Sons: New York, 1967.
(37) Klumbies, H.; Muller-Meskamp, L.; Monch, T.; Schubert, S.; Leo, K. The Influence of Laterally Inhomogeous Corrosion on Electrical and Optical Calcium Moisture Barrier Characterization. *Rev. Sci. Instrum.* **2013**, *84*, 024103.
(38) Nissen, D. A. Low-Temperature Oxidation of Calcium by Water Vapor. *Oxid. Met.* **1977**, *11*, 241−261.